

Interfacial Structure in Polymer Mixtures below the Critical Point

Utsawa K. Chaturvedi,^(a) Ullrich Steiner, Omer Zak, Georg Krausch,^(b) and Jacob Klein

Polymer Research Department, Weizmann Institute, Rehovot 76 100, Israel

(Received 20 March 1989)

The interfacial composition profile between two polymer phases at temperatures below the upper critical solution point has been measured directly, using an ion-beam method based on nuclear reaction analysis. The interface width grows with time to a finite limiting value. The variation of the limiting interfacial width as the critical temperature is approached from below is in quantitative accord with mean-field theories.

PACS numbers: 61.16.Fk, 68.10.-m, 68.35.Fx

Binary polymer mixtures are characterized by an inaccessible upper critical solution temperature, and will segregate at lower temperatures into two coexisting phases separated by an interfacial region.^{1,2} Likewise, two different polymers in contact do not in general interdiffuse freely, and an interfacial zone of finite width w separates them at equilibrium.³⁻⁶ This immiscibility is a fundamental consequence of the large chain size, which results in a very small combinatorial entropy of mixing, which scales as $1/N$, where $N \cong 10^3-10^4$ is the degree of polymerization. The (usually unfavorable) molecular interactions between unlike molecules, on the other hand, are N independent and remain comparable to those in analogous small molecule mixtures, in accord with regular solution theory.² The interfacial width w between the immiscible polymer phases arises from limited interpenetration of the chains, and controls properties such as polymer bonding, rheology of phase-separated blends, and the microstructure of block copolymers;⁶ a detailed knowledge of the profile has implications for the thermodynamics of polymer mixing, especially near the critical point where w diverges.

The composition profile $\phi(z)$ in the direction z normal to the interface between two immiscible polymers A and B with degrees of polymerization N_A and N_B , and local volume fractions $\phi_A \equiv \phi(z)$ and $\phi_B = 1 - \phi_A$, has been calculated by Helfand and co-workers³ and by others.⁴⁻⁶ The interfacial region at equilibrium below the critical temperature straddles the composition range between two coexisting phases, with $\phi_A = \phi_1$ and $\phi_A = \phi_2 < \phi_1$, and the profile is given by

$$\phi(z) = \frac{1}{2} \{(\phi_1 + \phi_2) + (\phi_2 - \phi_1) \tanh(z/w)\}. \quad (1)$$

The interfacial width w has been calculated as

$$w = \frac{a\sqrt{2}}{3\chi_c^{1/2}} \left(\frac{\chi}{\chi_c} - 1 \right)^{-1/2}, \quad \chi \geq \chi_c, \quad (2)$$

where a is the size of a statistical segment on the chain and χ is the Flory-Huggins interaction parameter; $\chi k_B T$ is the net interaction energy between a segment of A and one of B , where k_B is Boltzmann's constant and T the

absolute temperature. χ_c is the value of χ at the critical temperature T_c : In the Flory-Huggins mean-field model of polymer mixing,² $\chi_c = (N_A^{1/2} + N_B^{1/2})^2 / 2N_A N_B$.

Information on the interfacial region between immiscible polymer phases has come from indirect studies of properties such as interfacial tension.⁷ More recently, data from studies of small-angle x-ray^{8,9} and neutron scattering,¹⁰ and neutron reflectometry,¹¹ from phase-separated block copolymers and polymer blends, have been interpreted as indicating interfacial widths w consistent with Eq. (2) for both strong^{8,9} ($\chi \gg \chi_c$) and weak¹⁰ ($\chi > \chi_c$) incompatibility. Here we report the first *direct* measurements of the profile $\phi(z)$ and its limiting interfacial extent w , and the variation of w as the critical temperature is approached for $T < T_c$. Our data show explicitly that w changes in accord with the mean-field prediction (2). The development of the interfacial region with time is rather different from the case of free interdiffusion: Following an initial rapid interpenetration, it grows slowly to the limiting width w .

In this work we determine the profile $\phi(z)$ at the interface between deuterated polystyrene, dPS (sample A in Table I), and protonated polystyrene, pPS (sample B in Table I). The recent studies by Bates and co-workers¹² have demonstrated that mixtures of deuterated and of protonated analogs of the same polymer are characterized by a small value of the interaction parameter χ , resulting from slight differences between the isotopically

TABLE I. Characteristics of polystyrene molecules.

Sample	Degree of polymerization (weight averaged)	Polydispersity ^b
A , dPS ^a	$N_A = 9196$	1.30
B , pPS ^a	$N_B = 27788$	1.09
C , pPS ^a	$N_C = 8654$	1.08

^aObtained from Toyo Soda, Ltd., Japan, and characterized by them using light scattering and size-exclusion chromatography.

^bThe polydispersity is the ratio of the weight-averaged degree of polymerization to its number average. A value of 1 corresponds to a monodispersed sample.

differing segments.¹² For mixtures of dPS and pPS this interaction varies with temperature as¹² $\chi = (0.20 \pm 0.01)/T - (2.9 \pm 0.4) \times 10^{-4}$, so that for the values N_A and N_B of our polystyrene samples (Table I) the critical temperature T_c for phase separation is predicted to be around 200°C. Here we study the interface at temperatures *below* this critical point, though still considerably above the glass transition temperature of the polymer¹³ ($T_g \cong 100^\circ\text{C}$, that is, in conditions where the two polymers would unmix spinodally.²

In our experiments a thin film (~ 200 – 250 nm) of pPS is spin cast from toluene onto a polished silicon wafer, and a similarly cast dPS film is floated and laid on top to form a bilayer. The interface between the two polymers broadens on heating the bilayer to a temperature above T_g , as the molecules interpenetrate; the experiment is quenched following different times, and the interfacial profile is determined. The relevant spatial scales are some tens of nanometers. To access these, the concentration distribution of the deuterated chains is monitored using an ion-beam technique based on nuclear reaction analysis.¹⁴ This method¹⁵ complements previously used direct profiling techniques,¹⁶ and in particular it provides the high depth resolution necessary in the present study. In this approach a 700-keV ^3He beam impinges at a grazing angle of 15° on the top (deuterated) polymer layer, and penetrates into the lower layer through the interface. The reaction



emits energetic α (i.e., ^4He) particles which are detected at a forward angle (30°) and whose energy spectrum is stored in a multichannel analyzer. This spectrum contains information on the depth distribution of the deuterium (^2H) atoms in the sample. The incident ^3He particles lose energy by inelastic electronic processes as they penetrate the bilayer, which results in a much reduced energy of the emitted α particles deeper in the sample relative to those generated at the surface. Further energy losses occur as the emitted α particles travel through the sample to the surface on their way to the detector. The energy of the α particles reaching the detector thus provides a measure of the depth at which they were emitted by the nuclear reaction, and their energy spectrum is readily analyzed (in terms of the calibrated energy loss and reaction cross section) to yield the corresponding concentration versus depth profile.¹⁵ Our spatial resolution in profiling ^2H is limited by the detector resolution, by its acceptance solid angle, and by surface roughness of the sample: It is some 14 nm HWHM at the top (dPS) surface and ~ 20 nm at the bilayer interface.

In Fig. 1(a), the energy spectra of dPS/pPS bilayers are given both prior to annealing and following annealing at 160°C for a time $t = 2.61 \times 10^5$ s (all annealing carried out under vacuum). Figure 1(b) shows the corresponding composition versus depth profiles of the two

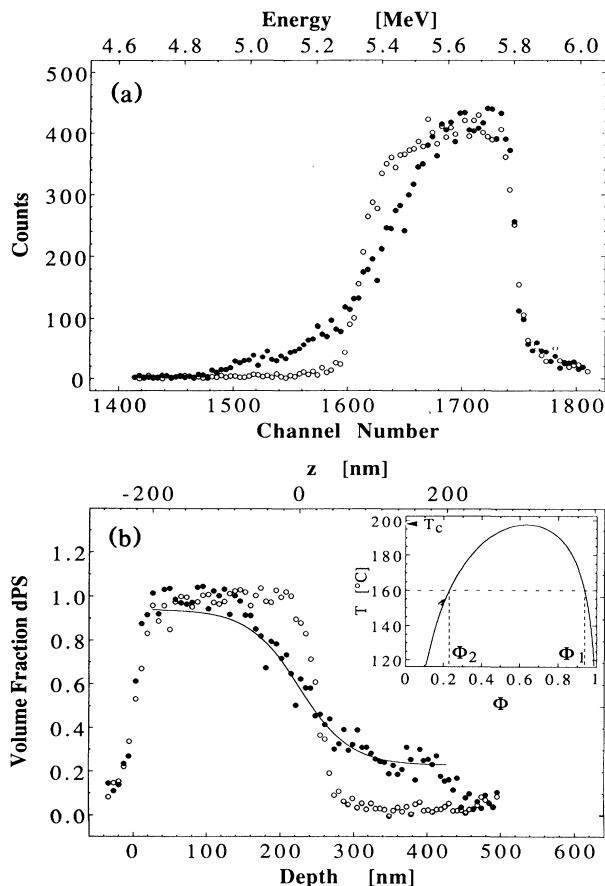


FIG. 1. (a) Energy spectra of α particles emitted from dPS (polymer A)-pPS (polymer B) bilayers prior to annealing (O) and following annealing for 2.61×10^5 s at 160°C (●). (b) The concentration-depth profiles corresponding to the unannealed and annealed spectra of (a) (for this annealing time the interfacial half width w' has already attained its limiting value). The solid curve $\phi(z)$ (scale on top axis) is Eq. (1), with ϕ_1, ϕ_2 calculated from the coexistence curve (inset) based on the Flory-Huggins model (Ref. 2) of mixing with the appropriate values of N_A, N_B , and $\chi(T)$. The dPS volume fraction at the polymer-air interface is normalized to $\phi=1$ for all profiles. The drop in the dPS concentration at depth ~ 420 nm occurs at the silicon substrate surface on which the bilayer is mounted.

samples, showing clearly the broadening at the dPS/pPS interface. The interfacial width w in Eq. (1) is related to the experimentally measured profile “half width” w' defined by

$$w' = \frac{1}{2} \left(\frac{d\phi}{dz} \right)_{\max}^{-1}, \quad (3)$$

where $(d\phi/dz)_{\max}$ is the slope over the region of the interface where $\phi(z)$ varies most rapidly, derived from the experimental profiles using a least-squares fit. From Eq.

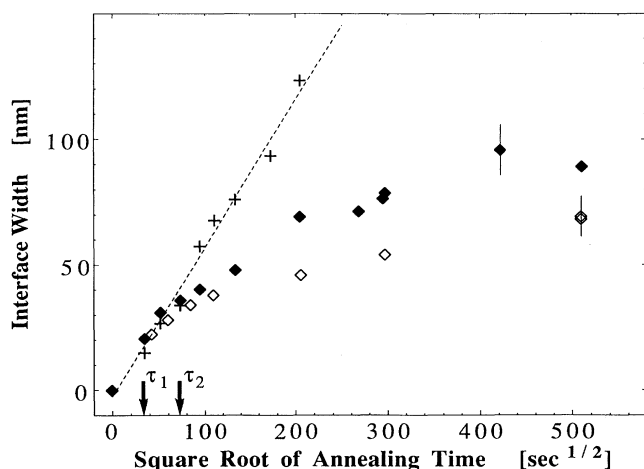


FIG. 2. The variation with annealing time of the interfacial width in the dPS-pPS bilayers. The width plotted is $(w'^2 - w_0^2)^{1/2}$, with w' defined as in the text, and with w_0 its mean value (20 nm) prior to annealing. The symbols are for annealing temperatures 150°C (\diamond) and 160°C (\blacklozenge) in the A/B bilayer, and 160°C (+) in the A/C bilayer. τ_1 and τ_2 correspond to the reptation times τ_{rep} of the dPS component (polymer A) at 150°C and 160°C, respectively (Ref. 18).

(1), which applies at equilibrium, i.e., at the limiting value of w' , we have $w = (\phi_1 - \phi_2)w'$. The solid line [Fig. 1(b)] is the full profile $\phi(z)$ from Eq. (1): ϕ_1, ϕ_2 are taken from the coexistence curve [inset to Fig. 1(b)], while w is derived from the measured w' .¹⁷

The development of w' with time at different temperatures $T < T_c$ is monitored and shown (for temperatures 150°C and 160°C) in Fig. 2 (corrected by quadratic subtraction for the small finite width at $t=0$ arising from instrumental resolution). We see clearly how the profile half width increases at short time but then levels off to its limiting value. The arrows in Fig. 2 mark the intrinsic molecular relaxation times (or reptation times²) τ_{rep} that the entangled dPS chains would have in their own melt,¹⁸ showing that the characteristic time to equilibrium for interfacial mixing at each temperature is appreciably larger than the corresponding τ_{rep} in the conditions of our experiments. A more detailed examination of the time variation indicates that, following an initial rapid increase, w' varies as a power of t markedly slower than $t^{1/2}$, until it eventually levels out at its limiting value at sufficiently long times. These observations emphasize the complexity of the interfacial development kinetics¹⁹ at $T < T_c$, and are currently being investigated in greater detail.

As a control, we monitored the development of w' with time under identical conditions (at 160°C) in a dPS/pPS bilayer where the pPS chains (sample C in Table I) had a lower degree of polymerization N_C ; consequently the annealing temperature is *higher* than the predicted critical temperature of $\sim 115^\circ\text{C}$ for the N_A/N_C system. The

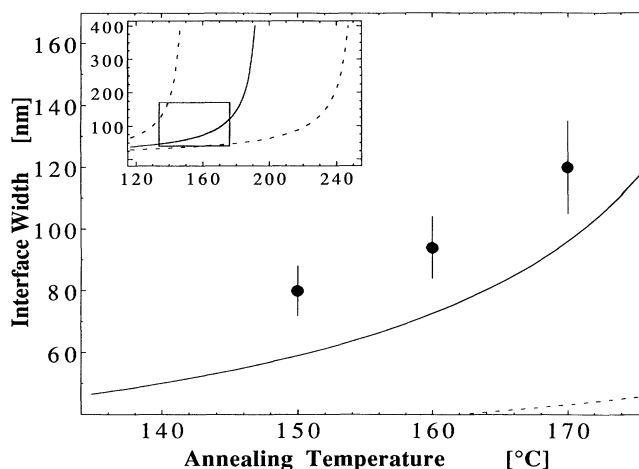


FIG. 3. The mean-field predicted variation of $w/(\phi_1 - \phi_2)$ with temperature (solid curve), from Eq. (2), based on $\chi(T) = (0.20 \pm 0.01)/T - (2.9 \pm 0.4) \times 10^{-4}$. The experimental points are the limiting values of w' taken from plots as in Fig. 2. Inset: Plot on a reduced scale, with the broken curves corresponding to the uncertainty limits implied by those in $\chi(T)$; shaded rectangle shows the range of the main plot.

development of w' in this case is also shown in Fig. 2, and is in marked contrast to the $T < T_c$ case: Here we see clearly the monotonic increase in w' expected for unrestricted interpenetration, with no indication of leveling off at long times. The broken line is the $w' \propto t^{1/2}$ variation expected for free interdiffusion. Our control measurements agree quantitatively with the recent study by Green and Doyle²⁰ of mutual diffusion in the dPS/pPS system at $T > T_c$ [within the uncertainty in $\chi(T)$ when thermodynamic slowing down is accounted for].

Finally, we examine the mean-field prediction for w from Eq. (2) for different temperatures [i.e., at different $\chi(T)$ values] as we approach T_c from below. This is shown in Fig. 3 where the experimentally determined limiting profile widths w' , obtained from plots such as Fig. 2, are plotted against the temperature. The solid line is the predicted variation $w' = w(\phi_1 - \phi_2)^{-1}$, with w evaluated from Eq. (2) taking $a = 6.6 \text{ \AA}$,¹⁴ while ϕ_1, ϕ_2 are obtained from the coexistence curve [see inset to Fig. 1(b)]. Within the spread implicit in the uncertainty of $\chi(T)$ (see inset to Fig. 3), the measured interfacial width is in good quantitative agreement with the mean-field predictions.

In summary, using a high-resolution ion-beam technique based on nuclear reaction analysis, we have succeeded in measuring directly the composition profile at the interface between two polymers at temperatures below the critical temperature for phase separation, and have shown that it grows with time to some finite limiting value of the interfacial width at sufficiently long

times. The variation of the interfacial width as the critical temperature is approached from below is in quantitative accord with the prediction of mean-field theories.

We are grateful to L. J. Fetters for donating one of the polymer samples used in this work, and we thank P. G. de Gennes, E. J. Kramer, and P. Pincus for helpful discussions, and G. Schatz for useful advice and encouragement. We also thank the technical staff of the accelerator laboratory for dedicated service, and D. Frohman (Intel Electronica Ltd., Israel) for donating the silicon wafers. This work was supported by the U.S.-Israel Binational Science Foundation and by the German-Israeli Foundation for Scientific Research and Development (GIF).

^(a)Present address: FBLJA World Laboratory Project, CERN, CH-1211, Geneva, Switzerland.

^(b)On leave from University of Konstanz, Konstanz, Federal Republic of Germany.

¹*Polymer Blends*, edited by D. R. Paul and S. Newman (Academic, New York, 1978).

²P. G. de Gennes, *Scaling Concepts in Polymer Physics* (Cornell Univ. Press, Ithaca, 1985).

³E. Helfand and Y. Tagami, *J. Chem. Phys.* **56**, 3592 (1971); E. Helfand and A. M. Sapse, *ibid.* **62**, 1327 (1975).

⁴P. G. de Gennes, *J. Chem. Phys.* **72**, 4726 (1980); P. Pincus, *ibid.* **75**, 1996 (1981).

⁵L. Leibler, *Macromolecules* **15**, 1283 (1982).

⁶K. Binder, *J. Chem. Phys.* **79**, 6387 (1983).

⁷R. J. Roe, *J. Colloid. Interface Sci.* **31**, 228 (1969); S. Wu, *J. Phys. Chem.* **74**, 632 (1970).

⁸T. Hashimoto, M. Fujimura, and H. Kawai, *Macromolecules* **13**, 1660 (1980).

⁹R. J. Roe, M. Fishkis, and J. C. Chang, *Macromolecules*

16, 1101 (1983).

¹⁰F. S. Bates, S. B. Dierker, and G. D. Wignall, *Am. Chem. Soc. Div. Polym. Chem. Prepr.* **28**(2), 32 (1987).

¹¹T. P. Russell, A. Karim, A. Mansour, and G. P. Felcher, *Macromolecules* **21**, 1890 (1988); M. L. Fernandez, J. S. Higgins, J. Penfold, R. Ward, C. Shackleton, and D. Walsh, *Polymer* **29**, 1923 (1988).

¹²F. S. Bates, G. D. Wignall, and W. C. Kohler, *Phys. Rev. Lett.* **55**, 2425 (1985); F. S. Bates and G. D. Wignall, *Phys. Rev. Lett.* **57**, 1429 (1986).

¹³*Polymer Handbook*, edited by J. Brandrup and E. H. Immergut (Wiley, New York, 1975).

¹⁴G. Amsel and W. A. Lanford, *Annu. Rev. Nucl. Part. Sci.* **34**, 435 (1984).

¹⁵U. K. Chaturvedi, U. Steiner, O. Zak, G. Krausch, and J. Klein (to be published).

¹⁶J. Klein, *Nature* **274**, 143 (1978); P. J. Mills, P. F. Green, C. J. Palmstrom, J. W. Mayer, and E. J. Kramer, *Appl. Phys. Lett.* **45**, 957 (1984); R. A. L. Jones, J. Klein, and A. M. Donald, *Nature* **321**, 161 (1986); J. Sokolov, M. H. Rafailovich, R. A. L. Jones, and E. J. Kramer, *Appl. Phys. Lett.* **54**, 590 (1989), and references therein.

¹⁷The measured values of w' and radius of gyration of the dPS chains are $\sim(10-20)\%$ of the bilayer thickness, so that finite-size effects are not expected to be significant.

¹⁸We take $\tau_{\text{rep}} = R_0^2/3\pi^2 D_{\text{rep}}$ [see M. Doi and S. F. Edwards, *The Theory of Polymer Dynamics* (Oxford Univ. Press, London, 1986)], where R_0^2 is the mean squared unperturbed end-to-end vector of the dPS chain (Ref. 14), while D_{rep} is the measured self-diffusion coefficient [P. F. Green, P. J. Mills, C. J. Palmstrom, J. W. Mayer, and E. J. Kramer, *Phys. Rev. Lett.* **53**, 2145 (1984)] of the dPS chains, taken at the appropriate temperatures.

¹⁹The related case of $\chi_c \ll \chi \ll 1$ is discussed by P. G. de Gennes, *C. R. Acad. Sci. (Paris)* **308**, Series II, 13 (1989).

²⁰P. F. Green and B. L. Doyle, *Phys. Rev. Lett.* **57**, 2407 (1986).